# Design and fabrication of PDMS-based electrostatically actuated MEMS cantilever beam

*Akanksha D. Singh* ✉, *Rajendra M. Patrikar*

*Centre for VLSI and Nanotechnology, Visvesvaraya National Institute of Technology, Nagpur 440010, India*
✉ *E-mail: akankshasingh222@gmail.com*

Published in Micro & Nano Letters; Received on 21st November 2019; Revised on 10th December 2019; Accepted on 20th January 2020

Polymer microelectromechanical system (MEMS) devices emerge as the new class of sensor devices for bio-sensing applications exhibiting high mechanical deformability and sensitivity. In this work, the design and fabrication of electrostatically actuated polydimethylsiloxane (PDMS) MEMS cantilever on flexible PDMS substrate is presented. The physical parameters of the cantilever were analysed and optimised using Taguchi method coupled with COMSOL Multiphysics software. This work focusses on the development of a novel approach for the simple and cost-effective fabrication process of PDMS cantilevers and subsequently its arrays. The proposed device consists of a PDMS body with the metal bottom electrode, PDMS anchor, and PDMS cantilever beam as its top electrode and immobilization surface. The work presented is of the cracking phenomenon in the metal layer sputtered on the PDMS substrate. The novelty of the fabrication process is the use of low-cost processes, no need for sophisticated lithography tools or etching equipment. Also, the process allows the use of alternate material as base substrate (glass, silicon wafer etc.) wherein it is not consumed and is reusable. The fabricated device is then electrically characterised for its pull-in characteristics.

**1. Introduction:** The cantilever-based microelectromechanical system (MEMS) devices have established themselves as a viable alternative solution to conventional assaying and diagnostic tools due to its better sensitivity, fast response time, compact size and cost-effectiveness [1–4]. Cantilever-based biosensing has shown tremendous growth for detection of explosives [5], DNA [6], bacteria [7], pesticides, environmental sensing etc.

The first step in the development of sensors is the design and optimisation of MEMS cantilever beam structure. It affects the device performance and hence factors like its geometry, dimensions, mode of operation, readout technique and materials must be determined. The MEMS cantilever beam can be operated in static or dynamic modes of operation [8]. In static mode, change in stress is measured due to deflection of the cantilever, whereas in dynamic mode, a shift in the resonant frequency is due to the added mass. Various readout mechanisms are available [9] and have to be selected depending on the nature of loading, the operating medium and the level of sensitivity required. The materials generally used for the fabrication of MEMS include silicon, polymer and metals.

A lot of research work has been focused on various aspects related to metal and silicon cantilevers. The polymers are now gaining particular interest in the research work due to their unique and diverse material properties, cost-effectiveness [10], comparatively simple structure processing [11–13] and their excellent biocompatibility.

Development of the polymer MEMS devices requires reconsideration of its design and fabrication with respect to conventional MEMS devices and their micromachining methods. This is attributed to its high mechanical deformation property. Also, it is significant to design microsystems that employ integrated actuation and readout mechanisms for improved portability. One such popular scheme is the electrostatic actuation and capacitive readout, wherein the two electrical contacts are used for actuation as well as sensing. It has been widely explored for Si-MEMS devices, whereas very few attempts [14] have been made in polymer MEMS devices.

Pioneering work in the field of polymer MEMS cantilever was done using SU-8 with optical [15], piezoresistive [16–19] readout techniques reporting improvement in device sensitivity for target detection. An emerging potential candidate for polymer microcantilevers is polydimethylsiloxane (PDMS). It is an inexpensive, transparent, biocompatible material with good thermal and chemical stability and adheres well to the surface of electronic materials [20–22]. It has a low modulus of elasticity ranging from 0.36 to 0.87 MPa depending on the ratio of the curing agent. There are few works on the use of PDMS for making either part [19] of or entire microcantilever beam [23–26]. The research on PDMS microcantilevers is still in the nascent phase, with various possibilities in the fabrication techniques, readout mechanisms currently being explored. There is no reported work utilising the electrostatic actuation for PDMS MEMS cantilever.

We report the first instance of design, optimisation and novel fabrication methodology of electrostatically actuated PDMS MEMS cantilever beam structure. This methodology can be extended to the fabrication of arrays of cantilever beams for the bio-assaying applications. This involves precision in the gap formed between the two electrodes, the formation of electrical contacts on the PDMS cantilever beam, etc. A classical fabrication approach to create a suspended beam structure consists of lithographic steps for patterning and etching. Etching of the layer usually makes the process expensive. In view of developing a simple and low-cost fabrication method, we have tried to take an alternative to both the steps. We have used a glass base substrate, which is reusable at the end of the fabrication process. The patterning is done using PTFE adhesive tape. We have utilised Aluminum foil as the sacrificial layer, which eliminates the etching step from the fabrication process, making it simpler. Also, we studied various aspects related to cracks induced due to metal sputtered on the PDMS substrate.

**2. Device design and operation:** In the static mode of operation, the electrostatically actuated MEMS cantilever device comprises a mechanical cum transduction platform, an actuation element and an immobilization layer. The actuation element is the bottom electrode, which acts as one of the electrodes for voltage actuation. The mechanical cum transduction platform is a multilayered structure, identified as follows as they appear from bottom to top: (i) top electrode (ii) structural layer (iii) electrical contact layer (iv) encapsulation layer. The top electrode facilitates the development of an




doi: 10.1049/mnl.2019.0728

electric field between itself and the bottom electrode whereas, the structural layer provides mechanical stability and acts as a stress collector. The electrical contact layer acts as a contact pad and forms electrical contact to the top electrode, while the encapsulation layer is used for the structure insulation.

The PDMS electrostatic MEMS cantilever beam comprises of a bottom actuation pad and an anchor on the flexible substrate, and a cantilever beam projecting from the anchor. The anchor and the bottom actuation pad consist of PDMS and metal layer, respectively. The cantilever beam consists of a PDMS layer as the structural layer sandwiched between the metal layers acting as the top electrode (below) and the electrical contact layer (above). The metal gets coated on the sides of the PDMS layer forming a contact between the alternate metal layers. Above the top metal layer, there is another layer of PDMS acting as an encapsulation layer. Thus, we get a four layered polymer–metal–polymer–metal structure at the free end of the cantilever beam. The bottom-most metal layer of the cantilever beam forms the top electrode of the entire structure. The schematic representation of the device is shown in Fig. 1.

The electrical biasing develops an attractive electrostatic force which causes the displacement of the top electrode leading to a change in capacitance. The voltage at which the top electrode touches the bottom electrode leading to the flow of current through the device is known as the pull-in voltage [27]. Pull-in voltage occurs when the beam traverses one-third of the total gap between the electrodes and happens due to the rapid increase of the non-linear electrostatic force than the linear spring restoring force. The pull-in voltage acts similar to the threshold voltage and can be used in sensor applications.

Miniaturised cantilever beam can be simply used as sensors in ambient environments with good sensitivity. For its use as a sensor, an immobilization layer is coated only on one side of the cantilever beam (preferably on the top) to guarantee the formation of differential surface stress. It is chemically modified and immobilised with receptor molecules specific for the target analyte. The chemical interaction reaction of the specific target molecule from the mixture of molecules with receptor molecules on the cantilever surface causes a change in its surface-free energy density due to change in its interaction between neighbouring receptor molecules. This produces a bending moment that is monitored as the deflection of the cantilever. This is depicted in Fig. 2. Depending on the development of compressive or tensile stress, the cantilever bends in the downward or upward direction [28], respectively. The deflection due to surface stress induced by adsorption is very small (in nm). Thus, the readout mechanism should be sensitive enough to capture such interactions.

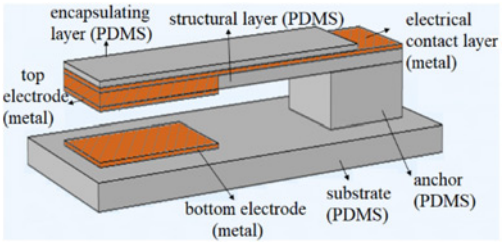


**Fig. 1** *3D schematic representation of multilayered MEMS cantilever beam*

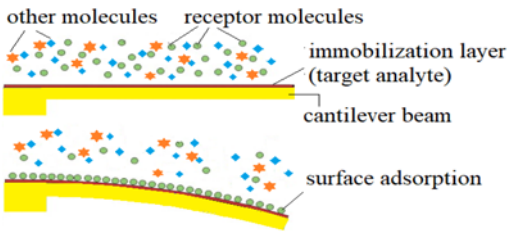


**Fig. 2** *Molecular-adsorption-induced bending of a cantilever beam*

For improved portability of the system, electrostatic actuation can be coupled with capacitive readout technique [29–31]. In this technique, depending on the downward or upward bending of the beam, the capacitance, either increases or decreases. This scheme offers good sensitivity and is mechanically simple and robust.

Another technique which can be utilised is the electrical readout mechanism [32] wherein the induced surface stress (from target–receptor interactions) is combined with electrostatic actuation mechanism to obtain final device deflection. The cantilever device is stressed with an applied voltage, whose value can be less than or equal to the pull-in voltage of the device depending on the nature of induced stress due to the interaction reaction. The resultant stress causes the cantilever beam to either touch the bottom electrode due to the pull-in instability regime or enable it to recover it from that regime. Thus, the pull-in voltage and the pull-in instability regime plays an important role in the sensing of receptor molecules. The current flow/discontinuity through the device upon a specific combination of induced stress and voltage applied is taken into consideration to estimate the final outputs.

The use of electrical readout mechanism in such cases is useful, wherein the induced surface stress can be combined with electrostatic actuation mechanism to obtain sensing. Pull-in voltage is the sensing parameter based on which different levels can be calibrated. The current flow through the device upon a specific combination of induced stress and voltage applied is taken into consideration to estimate the final outputs.

The key performance factor for electrostatically actuated MEMS cantilever is higher spring constant with lower actuation voltage. It can be improved by optimising the design parameters like device geometry, dimensions, material etc.

**3. Optimisation:** Optimisation was done using the Taguchi method [33] coupled with COMSOL Multiphysics followed by ANOVA analysis [34]. We selected nine control factors as shown in Table 1 with the three-factor level and adopted the L27 orthogonal array.

Based on the analysis, the following design parameters are selected:

Bottom electrode: 3000 μm × 3000 μm × 1 μm.
Gap: 22 μm.
Cantilever beam (bottom to top layers) include
Metal: 3000 μm × 3000 μm × 1 μm.
PDMS: 6000 μm × 3000 μm × 160 μm.
Metal: 6000 μm × 3000 μm × 1 μm.
PDMS: 6000 μm × 3000 μm × 12 μm.
Metal: Copper.

The multilayered MEMS cantilever beam with these design parameters was simulated in COMSOL Multiphysics using the

**Table 1** Control factors

| Sr. no. | Control factor |
|---|---|
| 1 | length of beam, μm |
| 2 | width of the beam, μm |
| 3 | thickness of structural PDMS layer, μm |
| 4 | thickness of PDMS layer (topmost), μm |
| 5 | length of metal layer (top electrode), μm |
| 6 | thickness of metal layer, μm |
| 7 | width of the bottom electrode pad, μm |
| 8 | Young's modulus of metal, GPa |
| 9 | gap between beam and bottom electrode, μm |

Electromechanics physics with stationary study to obtain its spring constant and pull-in voltage as 0.058 N/m and 2.5 V, respectively. Fig. 3 depicts the maximum displacement obtained at the voltage just before pull-in instability.

**4. Fabrication:** The fabrication process consists of two basic steps – patterning followed by deposition. Following are the key points of process:

- The MEMS cantilever device is fabricated on a glass base substrate. The use of any other alternative material for the base substrate is possible as the base substrate gets free after the fabrication and is reusable.

- The patterning at all layer levels is done by using PTFE thread seal tape on the unrequired portion to create patterns

- Use of Aluminum foil paper as the sacrificial layer, thus omitting the etching step, making the fabrication process low cost and simple.

The fabrication of multilayered PDMS cantilever is done in three parts namely, fabrication of bottom electrode and substrate, the multilayered beam followed by bonding the above two parts to form free-standing cantilever beam on the flexible substrate. Figs. 4–6 depict the schematic representation of step by step fabrication process steps utilised for device fabrication and is described as given below.

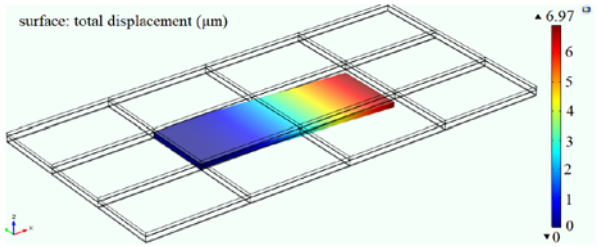


**Fig. 3** *Pull-in voltage analysis in COMSOL*

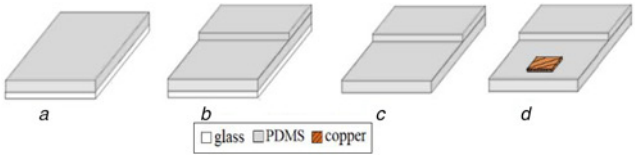


**Fig. 4** *Schematic step-wise process flow for Bottom electrode*
*a* Spin coat PDMS (flexible substrate) on glass
*b* Pattern and spin coat PDMS (Anchor)
*c* Peel off entire structure from the glass substrate
*d* Patterning and sputter deposition of Copper (bottom electrode)

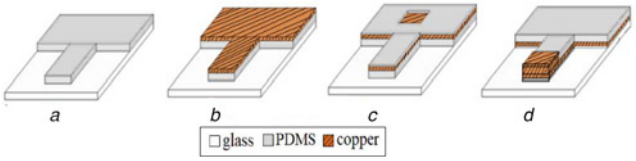


**Fig. 5** *Schematic step-wise process flow for beam*
*a* Spin coat and pattern PDMS (structural layer) on glass
*b* Patterning and sputter deposition of copper (Cu) (electrical contact)
*c* Patterning and spin coat of PDMS (encapsulation layer)
*d* Peel off, invert, pattern and sputter deposition of Cu (top electrode)

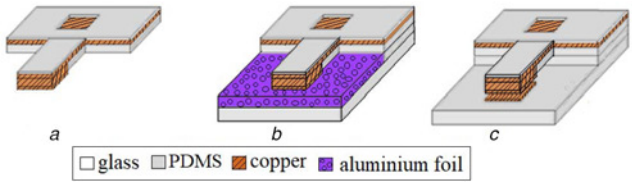


**Fig. 6** *Schematic step-wise process flow for bonding*
*a* Peel off from glass and invert to form PDMS beam
*b* Use of Aluminum foil as the sacrificial layer
*c* Removal of the sacrificial layer to form MEMS cantilever beam

Glass substrate is surface cleaned using isopropyl alcohol.

*Bottom electrode and substrate*: Surface cleaned glass square box is taken and a layer of PDMS (1 mm) is deposited by pouring the PDMS solution and curing it at 110°C for 50 mins as in Fig. 4*a*. Then, the anchor part of the cantilever beam is made by depositing the PDMS layer of thickness equal to the gap between the beam and bottom electrode. This is done by first patterning the substrate for anchor position by PTFE seal tape, followed by spin coating the PDMS. The PTFE tape is removed before curing the sample. It is as shown in Fig. 4*b*. The PDMS mold is now peeled off from the square box to get a flexible PDMS substrate and anchor on it as shown in Fig. 4*c*. The sample is patterned to form bottom electrodes. Copper is sputter deposited to obtain a thin layer of copper as shown in Fig. 4*d*.

*Beam*: A glass substrate is taken and on its reverse side, beam and anchor portions are sketched for chosen dimensions. The substrate is then surface cleaned on the front side and spin-coated with PDMS to act as the structural layer. The beam and anchor portion are cut using a razor cutter according to the sketch. The PDMS layer is first peeled off from the glass substrate and then placed on it again as shown in Fig. 5*a*. The sample is then sputtered for a thin film of copper to form the electrical contacts for the top electrode of the beam as shown in Fig. 5*b*.

The glass substrate is patterned in such a way that the side edges of the metal layer and the partial contact pad for the metal layer is kept covered. It is then spin-coated with a very thin layer of PDMS to form the encapsulation layer as shown in Fig. 5*c*. The multilayer structure is then peeled off from the glass substrate, inverted and fixed on the glass substrate using PTFE seal tape. It is patterned for the formation of the top electrode partially at the free end of the beam. Copper is sputter deposited to form the top electrode as shown in Fig. 5*d*. The sample is taken off and the tape is removed to get a four layered polymer cantilever, which is inverted to get top electrode as the bottommost layer of the polymer cantilever beam as shown in Fig. 6*a*.

*Bonding*: The bonding of the above two fabricated parts for the desired gap formation forms the crucial part. It is done at the anchor portion to form a free-standing structure. PDMS–PDMS bonding is done by spin coating thin layer over the anchor portion of the PDMS substrate. The portion covered with PTFE tape is replaced with a double layer of Aluminum foil (each with a thickness of 10.5 μm, which acts as the sacrificial layer. Then the multilayered beam structure is bonded to the anchor by hard pressing both the parts. It is then kept to cure for 4 mins to strengthen the bonding to form a structure as shown in Fig. 6*b*. Lastly, the cantilever beam is released by gently removing layer by layer the aluminum foil to get free standing cantilever beam structure as shown in Fig. 6*c*.

The following subsection describes in detail the methodologies for the preparation of different layers and analyses the layer interfaces.

4.1. PDMS layer: The main constituent of the polymer cantilever is PDMS, which is prepared as follows. A thin film of Sylgard 184 is used as a PDMS. It comes as an elastomer along with a




doi: 10.1049/mnl.2019.0728

cross-linking liquid (Hardener). A pre-cured solution of PDMS is prepared by mixing siloxane base and curing reagent in the ratio of 10:1. The prepared solution is degassed by putting it in a vacuum desiccator for about 25 min so that all the bubbles are gone from the solution. The PDMS mixture thus prepared is utilised within 25 min.

PDMS is the main constituent in electrostatic cantilever devices, wherein it acts as a substrate, anchor, structural layer and encapsulation layer. This requires its deposition having varying thickness for each layer. Thus, optimisation is required to obtain the desired value of thicknesses.

The spinning parameters are rotation speed, ramp time (to reach set speed) and the rotation time (at set speed). Table 2 shows the resulting thickness obtained by varying these parameters, which was measured by 3D Zeta microscope. Fig. 7 depicts the measured thicknesses of the anchor and structural layer. Also, the thickness can be expressed as a function of speed and time and can be estimated for any desired value.

4.2. Copper on PDMS layer: The electrical contact layer is needed to provide contact to the top electrode of the beam and for electrical probing of the device. Thus, we deposit copper on the PDMS structural layer to form the electrical contact layer. Copper is sputter deposited on the PDMS surface to obtain its thin film.

**Table 2** PDMS spinning parameters

| Sr. no. | Speed, rpm | Ramp time, s | Constant time, s | Measured thickness, µm |
|---|---|---|---|---|
| 1 | 750 | 23 | 35 | 165 |
| 2 | 1500 | 44 | 35 | 67 |
| 3 | 2200 | 61 | 35 | 37 |
| 4 | 3000 | 87 | 35 | 22 |
| 5 | 5000 | 145 | 35 | 12.3 |
| 6 | 7000 | 203 | 35 | 4 |

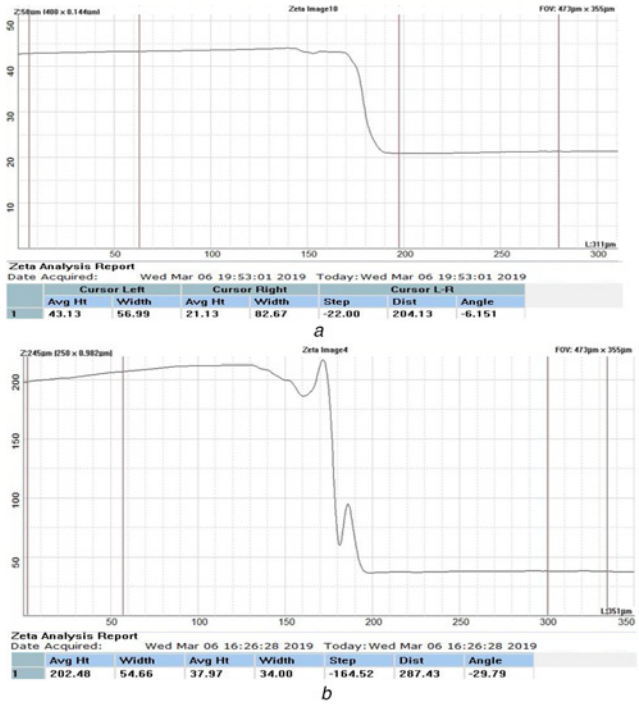


**Fig. 7** *PDMS thickness measurement for the gap of*
*a* 22 µm
*b* 165 µm

The substrate-bonded thin films behave in a different manner than the isolated thin-film layer. It is observed that metal thin film cantilevers can rupture/ break at its fixed end even with small applied strain. While for polymer-supported thin-films, the flexibility increases due to the polymer layer, facilitating the handling of larger strains and rupture at much longer elongations [35].

When the metal is sputter deposited on the PDMS substrate, thermal stresses are developed during and after metal deposition, which leads to the formation of the cracks thus limiting its conduction [36, 37]. This can be termed as process-induced cracking (PIC) [38], which occurs due to metallization. These cracks are mainly formed due to tensile stresses developed due to the melting point of the metal, substrate temperature, metal deposition rate etc. [39]. It is therefore desirable to initially study and investigate proper metal deposition conditions so that the cracks can be reduced.

Another type of cracking is associated with the post-process strain developed due to peeling of the metal deposited PDMS layer. This can be termed as the strain-induced cracking (SIC) [38]. One of our fabrication requirements is to peel-off the metal deposited PDMS layer to obtain a pattern. Thus, its study becomes crucial.

The PICs depend not only on the metallization related factors but also on elastomeric substrate deposition factor like the crosslinking time, ratio of base to curing agent. For the development of MEMS cantilever, the ratio of base to curing agent is kept fixed at 10:1 at a curing temperature of 110°C, which gives it less viscosity and proper elasticity.

We vary the crosslinking time of the sample as 10, 25, 50, 75 mins followed by metal sputtering for 20 min at 170 mA. The following micrographic images of cracks induced on metal surfaces are observed as in Fig. 8.

It is observed that the density of cracks increases with the increase in the crosslinking time. Also, from the measurement of crack widths, it is observed that the crack width increased with time. The reason is the increase in crosslinking within the PDMS layer causing the reduction in viscoelasticity and an increase in cracks.

The metal sputtered PDMS layer is then peeled off from the glass substrate and placed on it again. The micrograph images of the resulting surface as depicted in Fig. 9.

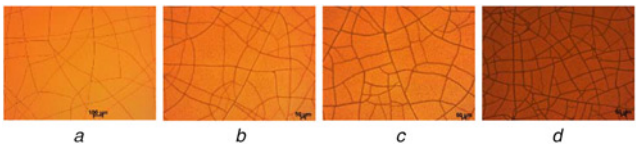


**Fig. 8** *PICs induced on the surface with the crosslinking time of*
*a* 10 min
*b* 25 min
*c* 50 min
*d* 75 min


**Fig. 9** *PICs along with SICs induced on the surface after peel-off with the crosslinking time of*
*a* 10 min
*b* 25 min
*c* 50 min
*d* 75 min

From Fig. 9, it is observed that SICs, depicted by thin lines within the PICs is maximum in the sample with the least curing time of 10 mins, whereas as crosslinking time increases, the SIC reduces and becomes thinner. This is due to the fact that with the increase in crosslinking time, the elasticity increases and hence increases the strain bearing capacity of the metal layer. This result is of special importance due to the fact that the cantilever beam bends on the application of voltage creating stresses on the beam. Layers with fewer SICs will be preferred over their counterparts. Hence, the crosslinking time should be chosen taking into consideration both the types of cracks.

In order to deal with the SIC, another set of experimentation was performed wherein; the cured PDMS samples were first peeled, then placed on the glass substrate again. Then, the samples were sputter-coated under the same initial conditions. Fig. 10 depicts the micrograph images obtained.

In this case, similar results are obtained, but the crack widths are reduced to a large extent as compared to its counterpart samples in Fig. 8. This behaviour results from the strain release of the PDMS layer when it is peeled off from the glass substrate. Thus, peeled off the PDMS layer helps to reduce the PICs widths and give a desirable surface.

From Fig. 11, it is observed that SICs still are formed similarly as previous ones, but are thinner than in Fig. 9.

Thus, from these two experiments and subsequent graphs as shown in Fig. 12, we analyse the effects of crosslinking time and peeling off (pre-/post-process) on the cracks induced on the metal surface. We conclude that the PDMS layer must be peeled off before sputtering metal to obtain a metal-PDMS layer with thinner cracks. The crosslinking time of PDMS is taken to be 50 mins as a trade-off between PICs and SICs.

Other experimentations (with pre-peel off) seeking the relation between deposition rate of metal versus the cracks induced were studied and it was found that the lower deposition rate led to a reduction in crack density and thinner cracks formation. The deposition rate was fixed at 155 mA current for 10 mins leading to a 1 µm thick metal layer.

Fig. 13*a* shows the zoomed image of the released cantilever structure with the bottom electrode on the PDMS substrate. Fig. 13*b* shows the zoomed image of the top view of the reverse side of the beam. Here the partially sputtered copper layer on the PDMS layer forms the top electrode of MEMS cantilever device structure. Fig. 13*c* gives the length and width of the fabricated beam.

**5. Electrical characterisation:** The fabricated devices are tested for current-voltage (*I–V*) measurements to obtain the pull-in voltage of the device. An electrical characterisation setup which consists of Karl Suss shielded probe station, source measurement unit (SMU) and Keithley 4200 Semiconductor characterisation system [40] was arranged.

*I–V* measurements were taken by applying the ramp voltage from 0 to 5 V between the bottom electrode and the top cantilever beam. For a set of straight cantilever beams, the current shoots up at a voltage of 2.4 V depicting a switching phenomenon as shown in Fig. 14. This is specified as the pull-in voltage for cantilever. At

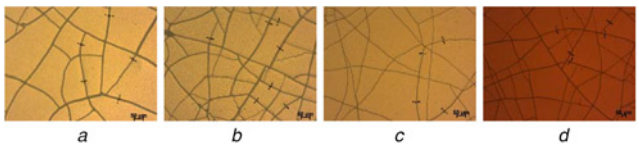


**Fig. 10** *PICs induced on the surface with pre-peel off of PDMS layer with crosslinking time*
*a* 10 min
*b* 25 min
*c* 50 min
*d* 75 min

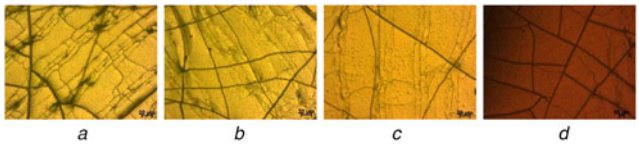


**Fig. 11** *PICs along with SICs induced on the surface after peel-off with crosslinking time of*
*a* 10 min
*b* 25 min
*c* 50 min
*d* 75 min

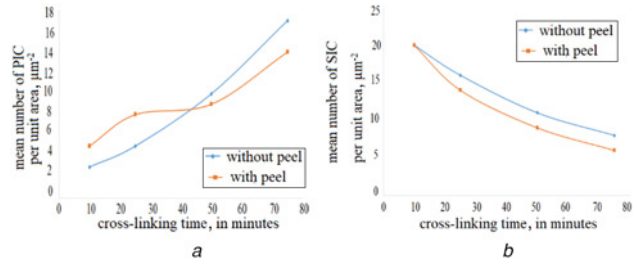


**Fig. 12** *Graph of crosslinking time versus*
*a* Mean number of PIC per unit area
*b* Mean number of SIC per unit area

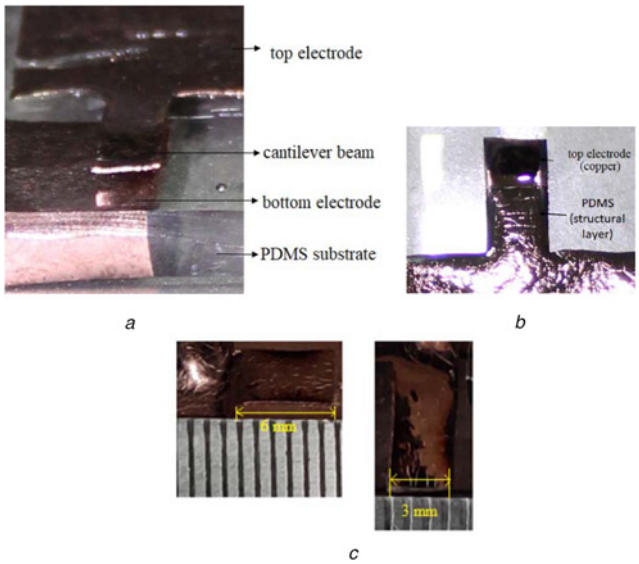


**Fig. 13** *Zoomed image of*
*a* Front view of released cantilever beam on PDMS substrate with the gap in between cantilever beam and bottom electrode
*b* Top view of the reverse side of the beam
*c* Device dimensions after measurement

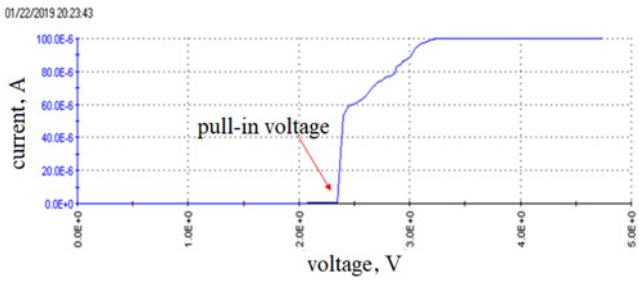


**Fig. 14** *I–V characterisation of fabricated device depicting pull-in voltage*




doi: 10.1049/mnl.2019.0728

this voltage, the beam snaps, causing cantilever and bottom electrode to come in contact and hence, set compliance value of current passes through the device. For device safety, compliance value is provided to prevent its breakdown.

Thus, we observe that even though the dimensions of the cantilever beam were slightly larger, the pull-in voltage of the device still remained in the range, which will be useful in many applications. This is mainly due to the use of polymer as the structural layer.

**6. Conclusion:** Polymer MEMS manifests to be a good alternative to the existing silicon MEMS for bio-sensing applications. In this work, we focused on PDMS MEMS cantilever device with electrostatic actuation operating in static mode. Its design and optimisation is done using Taguchi analysis coupled with the COMSOL Multiphysics. The MEMS beam was designed with the intention of having the higher restoring force and lower pull-in voltage so that the beam possesses better switching characteristics.

A high aspect ratio multilayered PDMS MEMS cantilever has been fabricated and tested. The low-cost processes were used for fabrication. Also, we have replaced the traditional etching process for the creation of a gap with the use of Aluminum foil as the sacrificial layer. This enabled the process to further become low cost and simpler. Study of process and SIC phenomenon to reduce the cracks on the metal sputtered PDMS layer is done. The electrical characterisation was performed and the analytical and simulated values were verified with the experimental results for pull-in voltage. These cantilevers can be used in various bio-sensing applications.

## 7 References


[1] Thundat T., Warmack R.J., Chen G.Y., *ET AL.*: 'Thermal and ambient-induced deflections of scanning force microscope cantilevers', *Appl. Phys. Lett.*, 1998, **64**, (21), pp. 2894–2896

[2] Lavrik N.V., Sepniak M.J., Datskos P.G.: 'Cantilever transducers as a platform for chemical and biological sensors', *Rev. Sci. Instrum.*, 2004, **75**, (7), pp. 2229–2253

[3] Boisen A., Thundat T.: 'Design and fabrication of cantilever array biosensors', *Mater. Today*, 2009, **12**, (9), pp. 32–38

[4] Stassi S., Fantino E., Calmo R., *ET AL.*: 'Polymeric 3D printed functional microcantilevers for biosensing applications', *ACS Appl. Mater. Interfaces*, 2017, **9**, (22), pp. 19193–19201

[5] Pinnaduwage L., Thundat T., Gehl A., *ET AL.*: 'Desorption characteristics of uncoated silicon micro-cantilever surfaces for explosive and common non-explosive vapors', *Ultramicroscopy*, 2004, **100**, (3–4), pp. 211–216

[6] Calleja M., Nordström M., Álvarez M., *ET AL.*: 'A highly sensitive polymer-based cantilever sensors for DNA detection', *Ultramicroscopy*, 2005, **105**, (1), pp. 215–222

[7] Longo G., Sarduy L.A., Marques Rio L., *ET AL.*: 'Rapid detection of bacterial resistance to antibiotics using AFM cantilevers as nanomechanical sensors', *Nat. Nanotechnol.*, 2013, **8**, (7), pp. 522–526

[8] Jensen J., Maloney N., Hegner M., 'A multi-mode platform for cantilever arrays operated in liquid', *Sens. Actuators B: Chem.*, 2013, **183**, pp. 388–394

[9] Vashist S.K.: 'A review of microcantilevers for sensing applications', *J. Nanotechnol.*, 2007, **3**, pp. 1–15

[10] Thuau D., Ducrot P.H., Poulin P., *ET AL.*: 'Integrated electromechanical transduction schemes for polymer MEMS sensors', *Micromachines. (Basel)*, 2018, **9**, (5), p. 197

[11] Kancharla V., Chen S.: 'Fabrication of biodegradable polymeric micro-devices using Laser micromachining', *Biomed. Microdevices*, 2002, **4**, (2), pp. 105–109

[12] Murali M., Yeo S.H.: 'Rapid biocompatible microdevice fabrication by micro- electro-discharge machining', *Biomed. Microdevices*, 2004, **6**, (1), pp. 41–45

[13] Ferrell N., Woodard J., Hansford D.: 'Fabrication of polymer microstructures for MEMS: sacrificial layer micro moulding and patterned substrate micro moulding', *Biomed. Microdevices*, 2007, **9**, (6), pp. 815–821

[14] Sousa P., Gutiérrez M., Mendoza E., *ET AL.*: 'Microelectromechanical resonators based on an all-polymer/carbon nanotube composite structural material', *Appl. Phys. Lett.*, 2011, **99**, (4), p. 044104

[15] Callega M., Tamayo J.: 'Low noise polymeric nanomechanical biosensors', *Appl. Phys. Lett.*, 2006, **88**, (11), p. 113901

[16] Rasmussen P.A., Thaysen J., Hansen O., *ET AL.*: 'Optimised cantilever biosensor with piezoresistive read-out', *Ultramicroscopy*, 2003, **97**, (1), pp. 371–376

[17] Johansson A., Blagoi G., Boisen A.: 'Polymeric cantilever-based biosensors with integrated readout', *Appl. Phys. Lett.*, 2006, **89**, (17), p. 173505

[18] Kale N.S., Nag S., Pinto R., *ET AL.*: 'Fabrication and characterization of a polymeric microcantilever with an encapsulated hotwire CVD polysilicon piezoresistor', *J. Microelectromech. Syst.*, 2009, **18**, (1), pp. 79–87

[19] Patkar R., Apte P., Rao V.R.: 'A novel SU8 polymer anchored low-temperature HWCVD nitride polysilicon piezoresistive cantilever', *J. Microelectromech. Syst.*, 2014, **23**, (6), pp. 1359–1365

[20] Zhou J., Ellis A.V., Voelcker N.H.: 'Recent developments in PDMS surface modification for microfluidic devices', *Electrophoresis*, 2010, **31**, (1), pp. 2–16

[21] Johnston I.D., Mccluskey D.K., Tan C.K.L., *ET AL.*: 'Mechanical characterization of bulk sylgard 184 for microfluidics and microengineering', *J. Micromech. Microeng.*, 2014, **24**, (3), pp. 10–11

[22] Chen J., Zheng J., Gao Q., *ET AL.*: 'Polydimethylsiloxane (PDMS)-based flexible resistive strain sensors for wearable applications', *Appl. Sci.*, 2018, **8**, (3), p. 345

[23] Nezhad A.S., Ghanbari M., Agudelo C.G., *ET AL.*: 'A new polydimethylsiloxane (PDMS) microcantilever with integrated optical waveguide for biosensing application'. Proc. SPIE 8412, Photonics North, 84120G, 2012

[24] Choi Y.S., Gwak M.J., Lee D.W.: 'Polymeric cantilever integrated with PDMS/graphene composite strain sensor', *Rev. Sci. Instrum.*, 2016, **87**, (10), p. 105004

[25] Holley M.T., Yekrang Safakar A., Maziveyi M., *ET AL.*: 'Measurement of cell traction force with a thin film PDMS cantilever', *Biomed. Microdevices*, 2017, **19**, (4), p. 97

[26] Kamat A.M., Pei Y., Kottapalli A.G.P.: 'Bioinspired cilia sensors with graphene sensing elements fabricated using 3D printing and casting', *Nanomaterials*, 2019, **9**, (7), p. 954

[27] Zhang W.M., Yan H., Peng Z.K., *ET AL.*: 'Electrostatic pull-in instability in MEMS/NEMS: A review', *Sens. Actuators, A*, 2014, **214**, pp. 187–218

[28] Mathew R., Sankar A.R.: 'A review on surface stress-based miniaturized piezoresistive SU-8 polymeric cantilever sensors', *Nano-Micro Lett.*, 2018, **10**, (2), p. 35

[29] Yamaguchi M., Kawamura S., Minami K., *ET AL.*: 'Distributed electrostatic microactuator'. Proc. IEEE Micro Electro Mechanical Systems Fort Lauderdale, FL, USA, 10 February 1993

[30] Dong J., Ferreira P.M.: 'Simultaneous actuation and displacement sensing for electrostatic drives', *J. Micromech. Microeng.*, 2008, **18**, (3), p. 035011

[31] Moore S.I., Reza Moheimani S.O.: 'Simultaneous actuation and sensing for electrostatic drives in MEMS using frequency modulated capacitive sensing'. Proc. 19th World Congress The Int. Federation of Automatic Control Cape Town, South Africa, August 24–29, 2014

[32] Kalambe J., Patrikar R.: 'Design, fabrication, and characterization of electrostatically actuated microcantilever sensor for temperature detection', *IEEE Sens. J.*, 2015, **15**, (3), pp. 1595–1601

[33] Ross P.: 'Taguchi techniques for quality engineering' (McGraw-Hill, New York, 1988)

[34] Khushalani D.G., Dubey V.R., Bheley P.P., *ET AL.*: 'Design optimization and fabrication of micro-cantilever for switching application', *Sens. Actuators, A*, 2015, **225**, pp. 1–7

[35] Lu N., Wang X., Suo Z., *ET AL.*: 'Metal films on polymer substrates strained beyond 50 percent', *Appl. Phys. Lett.*, 2007, **91**, (22), p. 221909

[36] Lacour S.P., Chan D., Wagner S., *ET AL.*: 'Mechanisms of reversible stretchability of thin metal films on elastomeric substrates', *Appl. Phys. Lett.*, 2006, **88**, (20), p. 204103

[37] Graz I.M., Cotton D.P.J., Lacour S.P.: 'Extended cyclic uniaxial loading of stretchable gold thin-films on elastomeric substrates', *Appl. Phys. Lett.*, 2009, **94**, (7), p. 071902

[38] Baëtens T., Pallecchi E., Thomy V., *ET AL.*: 'Cracking effects in squashable and stretchable thin metal films on PDMS for flexible microsystems and electronics', *Sci. Rep.*, 2018, **8**, (1), p. 9492

[39] Seghir R., Arscott S.: 'Controlled mud-crack patterning and self-organized cracking of polydimethylsiloxane elastomer surfaces', *Sci. Rep.*, 2015, **5**, p.14787

[40] 4200 SCS Semiconductor Characterization System Technical Data by Keithley Series 2400 Single channel Source Meter Instruments by Keithley